The Bulk Precipitation's Impact on Concentration Driving Force in Wax Deposition

Morten Siljuberg
Department of Petroleum Engineering & Applied Geophysics, NTNU
1/9/2012

ABSTRACT

In pipeline transportation of oil and condensate where the temperature of the surroundings are less than the inlet temperature, wax often precipitate out of solution and might deposit on the pipe wall. The main mechanism is considered to be molecular diffusion and its driving force is the concentration difference between the fluid in the bulk and near the wall. An anomaly from ordinary boundary layer conditions is caused by precipitation of wax in the bulk of the flow.

In this project, a review of 3 different methods for determination of molecular mass flux is done, where two are accounting for bulk precipitation and one does not.

Some interesting thoughts about considering bulk precipitation a competing phenomenon with deposition are also introduced. The concept is called bulk precipitation optimizing; bulk precipitation rate is considered an adjustable parameter, thus an optimizing can be done. It is based on the same principles as cold flow. A mathematically verification of the existence of an optimum and some discussion around its variables is done.

TABLE OF CONTENTS

1 INTRODUCTION 1

2 FUNDAMENTAL CONCEPTS 2

2.1 Wax deposition 2
2.1.1 Solubility, crystallization and WAT 2
2.1.2 Lateral temperature profile 2
2.1.3 Radial temperature profile and bulk precipitation 3
2.1.4 Concentration profile and molecular diffusion 3

2.2 Heat- and mass transfer theory 3
2.2.1 Convection 3
2.2.2 Radial transport in turbulent pipe flow 4
2.2.3 Heat- and mass transfer correlations 5
2.2.3.1 Turbulent pipe flow 5
2.2.3.2 External spherical flow 6

3 WAX PREDICTION METHODS FROM HEAT- AND MASS TRANSFER ANALYSIS 7

3.1 Independent heat and mass transfer method (IHMT) 7

3.2 Solubility method 7

3.3 Kinetic model/method 8
3.3.1 Quantifying the bulk precipitation rate 8
3.3.2 Precipitation rate constant k_r 8
3.3.3 Michigan wax predictor 9
3.3.4 Determination of k_r 9

3.4 Discussion 10

4 BULK PRECIPITATION OPTIMIZATION 11

4.1 Effects of convection coefficients 12

4.2 Impact of the flow rate 12

5 CONCLUSION 14

6 FIGURES 15

APPENDIX A DERIVATION OF THE SOLUBILITY METHOD 18

APPENDIX B TEMPERATURE DEPENDENCY OF VISCOSITY 19

APPENDIX C DIFFUSION COEFFICIENT AND ITS TEMPERATURE- AND VISCOCITY DEPENDENCY 20

7 BIBLIOGRAPHY 21

8 NOMENCLATURE 23

8.1.1 Abbreviations 24

8.1.2 Dimensionless numbers 24

1 INTRODUCTION

The worlds increasing thirst for oil, along with technological progress, has opened up for production and exploration in locations that earlier was not considered economically viable. The fields may be smaller and the environment may be colder and harsher. The use of subsea transportation of reservoir fluids has shown to be more efficient and because of colder environments arterial wax deposition in production and transportation equipment has become a bigger issue for the oil industry. There are several solutions to cope with the problem. Which one is best depends on the location, oil or condensates' composition, transport distance, surrounding temperature, WAT, etc. The pipeline can be isolated in order to lower the rate of heat loss, kinetic inhibitors can be injected to make the crystallization process slower or the wax can be scraped away regularly with a pig.

To establish an efficient wax remediation technique it is important to be able to forecast the rate of deposition and the deposits hardness (The latter is described with the concept of aging and is not the topic in this project). Especially in determination of pigging frequency this is essential. A too high remediation frequency will lead to unnecessarily high upkeep costs and too low frequency could lead to a stuck pig, which may shut down production causing loss of earnings for the operating company. In order to forecast the wax deposition simulation software is widely used. These are based on different wax deposition models which again is based on several physically principles, such as molecular diffusion, Brownian diffusion, particle agglomeration, gravity settling and shear dispersion. With the exception of molecular diffusion, all the above mentioned mechanisms are describing the radial transport of bulk-precipitated particles. It is still discussed whether these particles deposit on the wall or continue along with the flow. In this project, deposition of these particles is assumed not to happen. Hence, molecular diffusion enhanced by convective mass flux is the primary mechanism to cause wax deposition, and is the topic of this project. [1] Since pipeline transportation of hydrocarbons mainly takes place in turbulent flow, the focus has been on this flow condition.

2 FUNDAMENTAL CONCEPTS

2.1 WAX DEPOSITION

2.1.1 SOLUBILITY, CRYSTALLIZATION AND WAT

Precipitation of wax particles happens due to a reduction of the oil or condensates' ability to contain wax molecules when the temperature decreases; its solubility is reduced. WAT (wax appearance temperature) is a term used to describe the temperature beneath which the crystallization process begins. The solubility is a function of temperature and plots of solubility VS temperature is widely used in the process of quantifying wax deposition. Typical solubility curves are shown in Figure 1. It should be mentioned that using the term solubility for this case is a simplification. Wax consists of a variety of higher alkanes. Each of these components has its own solidification temperature and does therefore not precipitate out at the same temperature.

When the temperature in the oil or condensate sinks, the solubility goes down. When this solubility approaches the concentration of dissolved wax in the oil or condensate the WAT is reached. Because crystallization requires a supersaturation as a driving force, a further temperature reduction below the WAT is needed.

2.1.2 LATERAL TEMPERATURE PROFILE

As the oil or condensate flows through the pipeline, its heat gained in the reservoir is gradually lost by heat transfer to the surroundings. This creates a lateral temperature profile which is expressed by this equation [2]:

$$T_L(L) = T_u + (T_1 - T_u)\exp\left(\frac{-U\pi D}{\dot{m}C_p}L\right) \tag{1.1}$$

T_u is the ambient temperature, T_1 is the inlet temperature, U is the heat transmission coefficient, C_p is the oil or condensates' heat capacity and $\dot{m}$ is the mass flow rate in the pipe.

T_L represents the temperature of the flow at distance L from the inlet such that it is equal to T_m, which is the cross-sectional volumetric, temporal average of the flow [3, p. 473]:

$$T_m = \frac{2}{u_m r_p^2}\int_0^{r_p} u(r)T(r)rdr \tag{1.2}$$

For a turbulent flow the boundary layer at the wall is negligible small compared to the bulk. So T_L and T_m is often considered being the same as T_{core}. This is also assumed in this project.

In Figure 3 a typical temperature profile is illustrated together with deposition thickness after some weeks of operation. As we see from the figure, the deposition begins long before the WAT is reached. That is because the temperature in proximity to the wall reaches the WAT before the turbulent core does.

2.1.3 RADIAL TEMPERATURE PROFILE AND BULK PRECIPITATION

The nature of heat transport creates a radial temperature profile inside the pipe, as seen in Figure 2. This temperature profile decides at which radial position the WAT is reached and thus where the crystallization process can start. Deposition of bulk precipitated wax particles requires a transport mechanism towards the wall if they are to deposit. If such a transport mechanism does not exist, bulk precipitation is considered a competing phenomenon with deposition. [4] Thus, only wax molecules precipitated in immediate proximity to the wall is considered to contribute to the deposit growth. This is an important feature that influences the concentration driving force, hence also the deposition rate, as we will see later on.

2.1.4 CONCENTRATION PROFILE AND MOLECULAR DIFFUSION

Because the solubility of wax is a function of temperature, the temperature profile is influencing the concentration profile of dissolved wax. This is an important particularity that makes ordinary heat- and mass transfer analogies unavailing, since these require ordinary boundary layer profiles, where the concentration profile is established independently.

As wax precipitate out of the solution, the concentration of dissolved molecules decreases. This produces a driving force for molecular diffusion which again leads to a radial concentration profile in the pipe. Figure 4 shows an illustration of this. As seen here, the concentration gradient does not start before the WAT is reached.

2.2 HEAT- AND MASS TRANSFER THEORY

A usual way of describing a flow in physics is by consider a driving force and either a coefficient reflecting the materials reluctance to contribute to the flow, or the inverse, a willingness coefficient. An example is convective heat and mass transfer. Convection is a transport mechanism driven by both conduction (diffusion) and advection (bulk motion of fluid). In this project, the mass transfer rate of dissolved wax molecules from the bulk to the pipe wall is investigated, which is a typical convection problem.

2.2.1 CONVECTION

A central equation quantifying the convective heat transfer is Newton's law of cooling, which not only can be used to determine the heat transfer, but also mass transfer:

For heat transfer:

$$q'' = h(T_s - T_m) \tag{1.3}$$

For mass transfer:

$$n'' = h_m(C_s - C_m) \tag{1.4}$$

T is temperature, C is concentration and their subscripts s and m denotes the property at the surface and bulk average, respectively. q'' and n'' represent heat- and mass flux per unit area, respectively. To find these quantities we need to know the convective coefficients h and h_m. Finding these coefficients is often referred to as "the problem of convection". Theses coefficients are dependent on variables such as fluid properties, surface geometry and flow conditions. To simplify the analysis, there has been defined a set of dimensionless numbers that represents flow conditions and fluid properties. Most commonly, these non-dimensional quantities are

determined by preforming empirical experiments. Definitions and description of the dimensionless numbers used in this project is found in the Nomenclature.

In a fully developed pipe flow the convective coefficients are constant in the flow direction. [3] For an oil or condensate transporting pipeline with wax deposited on the walls, this is not true.

2.2.2 RADIAL TRANSPORT IN TURBULENT PIPE FLOW

Pipeline transportation of oil and condensate does in most cases operate under turbulent flow conditions. The quantifying equations described in this project will therefore apply to these conditions.

In a fully developed turbulent pipe flow, i.e. far enough from the inlet, we distinguish between 3 different radially segregated regions of the flow:

1. Laminar sublayer
2. Buffer Layer
3. The turbulent core

In the laminar sublayer transport processes is dominated by diffusion. In the buffer layer transport by diffusion and turbulent mixing are of the same order of magnitude. And in the turbulent core the turbulent mixing is the dominant and the diffusion is negligible.

Quantification of the mass and heat transport can in all these layers be done with Fick's and Fourier's law, modified to also represent the turbulent mixing: [5, p. 404] [5, p. 467]

$$q'' = -(k_f + \varepsilon_h)\frac{dT}{dr} \quad \text{(Fourier's law)} \tag{1.5}$$

$$n'' = (D_{AB} + \varepsilon_m)\frac{dC}{dr} \quad \text{(Fick's law)} \tag{1.6}$$

Where k_f is the thermal conductivity and D_{AB} is the binary diffusion coefficient.

The mass- and heat eddy diffusivities, ε_H and ε_M , is defined by: [5]

$$\frac{\varepsilon_m}{D_{AB}} \equiv \frac{Sc}{Sc_T}\frac{\varepsilon}{\nu} \tag{1.7}$$

$$\frac{\varepsilon_h}{k_f} \equiv \frac{\Pr}{\Pr_T}\frac{\varepsilon}{\nu} \tag{1.8}$$

Where ε is the momentum diffusivity and is found from the following equation: [6]

$$\frac{\varepsilon}{\nu} = (\kappa y^+)^2 \left[1 - \exp\left(\frac{-y^+}{A} \right) \right]^2 \left| \frac{dV_z^+}{dy^+} \right| \tag{1.9}$$

κ and A are constants for the correlation of eddy viscosity and is equal to 0.4 and 26 respectively. y^+ and V_z^+ is the non-dimensional wall normal distance and velocity, normalized by u_τ. u_τ is the friction velocity and is defined by:

$$u_\tau = \sqrt{\frac{\tau_w}{\rho}} \tag{1.10}$$

Where τ_w is the wall shear stress and ρ is the fluids density.

In the core, turbulent mixing, eddies and vortices make the mixing in radial direction so big that the gradients is negligible. Therefore a constant concentration and temperature from the pipe center to a point located at a representative radial distance close to the wall is reasonable; here, the eddy diffusivities are becoming sufficiently low. From this point towards the wall, the temperature- and concentration gradient becomes significant. The point is located at the division between buffer layer and log-layer.

2.2.3 HEAT- AND MASS TRANSFER CORRELATIONS

Considering the fundamentals equations of mass-, energy- and momentum conservation together with the theory about their respective boundary layers, it has been found that there exists similarity between transportation of these properties. These analogies are expressed by correlations between their respective dimensionless convection coefficients numbers. For different geometries and flow conditions we have different correlations. We are mainly interested in correlations for turbulent, cylindrical pipe flow, but for the crystallization process of individual wax crystals a correlation for flow towards a spherical particle is also used.

2.2.3.1 Turbulent pipe flow

For turbulent pipe flow, there has been developed several correlations for heat- mass- and momentum transfer. One of these is the Dittus-Boelter correlation, which gives us the dimensionless convective heat transfer coefficient for a given Reynolds- and Prandtl number:

$$\mathrm{Nu_D} = 0.023 \mathrm{Re_D}^{4/5} \mathrm{Pr}^{\mathrm{n}} \tag{1.11}$$

It has been shown that the Dittus-Boelter equation can give errors as large as 25%. [3, p. 492]
More accurate equations have therefor been developed, such as the:
Petukhov equation: [3, p. 492]

$$Nu_D = \frac{\left(\frac{f}{8}\right) \mathrm{Re}_D \, \mathrm{Pr}}{1.07 + 12.7 \left(\frac{f}{8}\right)^{1/2} (\mathrm{Pr}^{2/3} - 1)} \tag{1.12}$$

And the Gnielinski equation, which gives a correlation for smaller Reynold numbers: [3, p. 492]

$$Nu_D = \frac{\left(\frac{f}{8}\right)(\mathrm{Re}_D - 1000)\,\mathrm{Pr}}{1 + 12.7\left(\frac{f}{8}\right)^{1/2}(\mathrm{Pr}^{2/3} - 1)} \tag{1.13}$$

Correlations of the form that Petukhov and Gnielinski suggested can give an uncertainty of less than 10%, but because of its simplicity Dittus-Boelter is widely used. All these correlations are also applicable for mass transfer by replacing Nu_D and Pr with Sh_D and Sc, respectively. This is because the mechanisms governing mass transport are essentially the same as those governing heat transports. The concept is known as the "Reynolds analogy".

In the case where the pipe flowing fluid is cooled by the pipe walls, which is our case, the exponent n in equation (1.11) is equal to 0.3 [3, p. 491]. We then obtain the following equations:

For heat transfer

$$\mathrm{Nu_D} = 0.023\mathrm{Re_D}^{0.8}\mathrm{Pr}^{0.3} \tag{1.14}$$

For mass transfer

$$Sh_\mathrm{D} = 0.023\mathrm{Re_D}^{0.8}\mathrm{Sc}^{0.3} \tag{1.15}$$

By combining these two equations we can also obtain correlations between the dimensionless convective heat and mass transfer coefficients:

$$\frac{Sh_D}{Nu_D} = \left(\frac{Sc}{\mathrm{Pr}}\right)^{1/3} = Le^{1/3} \tag{1.16}$$

It should be commented that (1.11), (1.13) and theirs analogue mass transfer equations only pertain for smooth pipes. The transfer rates become bigger with increasing roughness and the effect are discussed by Bhatti and Shah. [7]

2.2.3.2 External spherical flow

A numerous mass- and heat transfer correlations has been suggested for external spherical flow. Ranz and Marshall proposes the following: [3, p. 415]

$$Sh_D = 2 + 0.6\,\mathrm{Re}_D^{1/2}\,Sc^{1/3} \tag{1.17}$$

When the particles is moving with the same speed and direction as the surrounding fluid the particle's Reynolds number is 0 and the Sherwood number for external spherical flow becomes 2.

3 WAX PREDICTION METHODS FROM HEAT- AND MASS TRANSFER ANALYSIS

In this chapter 3 different methods for determination of the convective mass flux is shown. The two first approaches involves finding the dimensionless convective mass transfer coefficient, Sh_D, from correlations from heat- and mass transfer analogies, it is then nondimensionalized from its definition (see Nomenclature) and the mass transfer rate is then calculated from the mass transfer's analogy to Newton's law of cooling, equation (1.4). The third approach uses numerical methods to solve fundamental energy- and mass conservation equations to obtain the mass flux.

3.1 INDEPENDENT HEAT AND MASS TRANSFER METHOD (IHMT)

Using heat- and mass transfer analogy for wax deposition modeling was first introduced by Singh et al. [8]. They were considering laminar flow and the correlations are a bit different than those for turbulent flow, which is shown here. For the IHMT-method Sh_D is found from equation (1.15).

This method assumes that no wax molecules will precipitate in the bulk. Thus, all the wax molecules will deposit on the wall. It would result in an overestimation of the deposition rate and the method calculates an upper limit for wax deposition due to molecular diffusion. It would be valid if WAT=T (wall), which might be valid for a small section of the pipe.

3.2 SOLUBILITY METHOD

A method that accounts for bulk precipitation is needed in order to determine the correct deposition rate. This was analyzed by Venkatesan et. al [9] . They suggested the following equation to obtain Sh_D, which is derived in Appendix A:

$$Sh_D = Nu_D \left(\frac{dC_{wo}(T)}{dT} \right) \frac{T_{bulk} - T_{wall}}{C_{w,bulk}(T) - C_{w,wall}(T)} \tag{3.1}$$

C_{wo} represents the solubility of wax in oil or condensate and is a function of temperature, $C_{w,bulk}$ and $C_{w,wall}$ is the concentration of wax in the oil or condensate at their respective places. Solubility curves as those shown in Figure 1, is used to obtain both the solubility gradient and the concentrations. The Nusselt number can be obtained from the Dittus-Boelter correlation since the temperature profile is independently established. The heat that the crystallization process provides might influence the profile, but is not considered in this project.

The solubility method assumes that wax will precipitate immediately as the solubility decreases. This is a simplification, since the crystallization process is not instantaneous. By overestimating the amount of precipitation in the bulk, the method underestimates the deposition rate by molecular diffusion. Hence, it represents a lower limit for the deposition rate due to molecular diffusion.

An advantage of this method is the direct expression for the convective mass transfer coefficient.

3.3 KINETIC MODEL/METHOD

The inertia in the crystallization process of wax particles needed to be accounted for in the determination of the mass flux by molecular diffusion. This is done by considering the kinetics of crystallization.

3.3.1 QUANTIFYING THE BULK PRECIPITATION RATE

As mentioned, the crystallization of wax molecules happens because the solubility of the oil or condensate deceeds[1] the concentration and a supersaturation is arose. The crystallization process is driven by a supersaturation, which is determined by the difference between the solubility C_{wo} and concentration C_w.

Huang Z. et. al [4] introduces the crystallization rate for bulk precipitation of wax quantitatively with the following equation:

$$G = k_r (C_w - C_{wo}(T)) \tag{3.1}$$

Where G is the the growth rate of precipitated wax particles per unit volume, k_r is the precipitation rate constant. The growths driving force is the supersaturation of dissolved wax molecules as explained.

3.3.2 PRECIPITATION RATE CONSTANT K_R

The precipitation rate constant k_r describes the crystallization speed quantitatively and is equated as:

$$k_r = k_d A_n \rho_n \tag{3.2}$$

Where A_n is the surface of the nucleus, ρ_n is the number density of the nuclei and k_d is the mass transfer coefficient to the particles. k_d is found from the definition of the Sherwood number. If we assume spherical particles and that they are moving with approximately the same speed as the fluid surrounding them, i.e particle Reynolds number is close to zero, equation(1.17) gives us $Sh_D(\mathrm{Re}_D = 0) \cong 2$. Together with the equation of surface area of a sphere:

$$A_n = \pi d_n^2 \tag{3.3}$$

The precipitation rate constant becomes equated as:[2]

$$k_r = 2\pi d_n \rho_n D_{wo}(T, \mu) \tag{3.4}$$

Obtaining a quantitative measure of d_n and ρ_n involves finding a solid-liquid thermodynamic equilibrium for the wax-oil system and is very complex. Hence, another approach is necessary to obtain a value of k_r.

---

[1] An antonym of the word exceed is often needed. The word deceed has been suggested, but is still not accepted by Oxford dictionaries.

[2] A mistake was done in the derivation of equation (3.4) in the original paper [4], the equation shown here is the correct.

k_r is a function of temperature and viscosity, and since viscosity is a function of temperature, k_r can be expressed as a function of just temperature. If k_r at a reference temperature is obtained we can use such a correlation to determine k_r at another temperature. Combinations of the empirical correlations in equation (B.3) and (C.2), described in Appendix B and Appendix C gives us a such correlation:

$$\frac{k_r}{k_{r,cloud}} = \left(\frac{T}{T_{cloud}}\right)^{1.47} e^{\frac{\gamma E}{R}\left(\frac{1}{T}-\frac{1}{T_{cloud}}\right)} \tag{3.5}$$

Here the cloud point is chosen as a reference temperature. If we assume that d_n and ρ_n are independent of the radial distance this means that if we have the precipitation rate constant at a given temperature, we can obtain it at any place in the pipe.

3.3.3 MICHIGAN WAX PREDICTOR

The concept of accounting the kinetics of precipitation in wax deposition was first considered by Huang et. al [4]. A wax deposition model called Michigan wax predictor (MWP) was developed. The model is using a stepwise method, considering the heat- and mass transport over a small fraction of the total transport length. The method differs from the heat-mass analogies, where we use empirical correlations to represent the total transport of heat and mass over the boundary layer. The shortened fundamental energy- and mass conservation equation used in the model are:

For heat transfer,

$$V_z \frac{\partial T}{\partial z} = \frac{1}{r}\frac{\partial}{\partial r}\left[r(\varepsilon_H + k_f)\frac{\partial T}{\partial r}\right] \tag{3.6}$$

For mass transfer

$$V_z \frac{\partial C}{\partial z} = \frac{1}{r}\frac{\partial}{\partial r}\left[r(\varepsilon_M + D_{wo})\frac{\partial C}{\partial r}\right] - G \tag{3.7}$$

Where V_z is the lateral velocity, z is the lateral position. We recognize the diffusion term from chapter 2.2.2. The eddy diffusivities is determined by equation (1.7) and (1.8). G is the growth rate of precipitated particles.

3.3.4 DETERMINATION OF K_R

A potential disadvantage with the model is that we have to obtain a value for the precipitation rate constant at a reference temperature. The determination can be done by comparing experimental data with simulations done with the method. The determination is done by doing simulations with the MWP with different k_r. An estimate of k_r is found when the deviation from the experimental results is minimized, see Figure 6.

3.4 DISCUSSION

As mentioned, the IHMT- and solubility method represents the upper and lower limit for wax deposition by molecular diffusion. The former do not account for bulk precipitation and the latter does. One way of understanding the difference between accounting for bulk precipitation or not is to see how the bulk precipitation influences the establishment of the concentration gradient. As seen in Figure 5, not accounting for bulk precipitation (IHMT-model) creates a steeper concentration gradient and the molecular diffusion becomes bigger. The opposite is true for accounting bulk precipitation (solubility-model).

Simulations show that the same deposition rate of these two methods can be obtained by adjusting k_r . The results from IHMT-method is obtained by setting $k_r = 0$ and for the solubility method, $\lim_{k_r \to \infty}$, for simulation purposes Singh et al [4] shows that 10^3 is sufficiently. For laminar flow conditions, $k_r = 0$ (IHMT-model), shows excellent correlation with the experimental results. [4]

Singh et. al [4] suggests that the precipitation rate constant is varying with the flow conditions and not the type of oil. He reports an indication that under turbulent flow conditions, values of the precipitation rate constant is 1.4. [4]. Unfortunately, he does not mention any dependency to the Reynolds number.

4 BULK PRECIPITATION OPTIMIZATION

Considering bulk precipitation a competing phenomenon with deposition introduces some interesting consequences. If this is true, bulk precipitation of wax particles would be advantageous and thus desired in order to minimize the deposition rate. If the amount of bulk precipitation can be regulated, bulk precipitation should be included in the optimization process of the pipe design.

Since the local amount of bulk precipitation is determined by how far the WAT radially penetrates into the pipe, it would be desired to keep the WAT as far (radially and lateral) in the pipe as possible.

Let us call the radial position of the WAT r_{WAT}. Since the temperature gradient, which decides where the WAT is reached, is determined by the heat loss at that particular distance L, r_{WAT} must also be a function of the local heat transfer rate, hence also the heat transfer coefficient. The temperature profile is strongly correlated to the momentum transfer too, which are determined by the Reynolds number, so the overall flow rate and pipe diameter must also be influencing variables.

We end up with:

$$r_{WAT}(L) = f(q_L(L), \dot{m}, D) \tag{4.1}$$

Where r_{WAT} is the radial position of the WAT and $q_L(L)$ is the local heat transfer rate per unit length, both at lateral position L. $\dot{m}$ is the pipe mass flow rate and D is the diameter.

Since the penetration depth of the WAT influences the amount of bulk precipitation per unit length at a given lateral position we have:

$$G_L(L) = f(r_{WAT}(L)) \tag{4.2}$$

Where $G_L(L)$ is the bulk precipitation per unit length, defined as:

$$G_L = \int_0^{D/2} G(r) P dr \tag{4.3}$$

G(r) is defined in (3.1) and P is the periphery. The total bulk precipitation in the pipeline is:

$$G_{tot} = \int_0^{L_{tot}} G_L(L) dL \tag{4.4}$$

Where P is the periphery. A possible positive effect on changing the flow rate cannot be evaluated by G_{tot} since an increase in flow rate will lead to a higher deposition potential. Hence, a ratio must be used; ratio of bulk precipitating wax particles to the mass flow rate:

$$f_G = \frac{G_{tot}}{\dot{m}} \tag{4.5}$$

Thus, f_G is a quantitative measure of the severity of bulk precipitation of wax, and if it is a competing phenomenon with deposition, an optimizing would be advantageous.

Of course, in an economical optimization process, other variables must be considered as well, such as and the cost of pipe, pumping, pigging, etc.

4.1 EFFECTS OF CONVECTION COEFFICIENTS

In order to not deplete the "wax-reservoir" in the bulk before the solubility approaches concentration a high heat transfer coefficient compared to mass transfer coefficient is desired. It will contribute to the penetration depth of r_{WAT} .

In ordinary boundary layers, where concentration profile is not dependent on the temperature profile, the equations (1.14) and (1.15) are used for determination. For our case, where the concentration gradient is dependent on the temperature profile, the relationship is a bit different. Since the MWP don't have any direct expression for the convective mass transfer coefficient, the equation from the solubility method is showed for illustration. Where the temperature profile is independently established, Dittus Boelter can be used be used for the Nusselts number:

$$\mathrm{Nu_D} = 0.023\mathrm{Re_D}^{0.8}\mathrm{Pr}^{0.3} \tag{4.6}$$

$$Sh_D = 0.023\,\mathrm{Re}_D^{\,0.8}\,\mathrm{Pr}^{1/3}\left(\frac{dC_{wo}(T)}{dT}\right)\frac{T_{bulk}-T_{wall}}{C_{w,bulk}(T)-C_{w,wall}(T)} \tag{4.7}$$

This equation is only valid for turbulent flow conditions. In the laminar and transition regime other correlations must be used. As seen here, the shape of the solubility curve must be considered for determination for a correct Sherwood number. Different solubility curves are shown in Figure 1, as we see here the gradient $\frac{dC_{wo}(T)}{dT}$ varies a lot for different oils. Intuitively, it will have a big impact on Sh_D and that a slight curve is preferred. But since the concentration difference $C_{w,bulk} - C_{w,wall}$ most often is strongly influenced by the solubility curve these two might equal each other out. Thus, a slight solubility curve is not necessarily an advantage. This is also indicated by Singh et. al. [4, p. 2960]

4.2 IMPACT OF THE FLOW RATE

Singh et al. reports that in laminar flow, bulk precipitation does not occur. It occurs when moving into the turbulent regime. [4] [8] A reason for that might be that the convective mass transfer coefficient is sufficiently large compared to the convective heat transfer coefficient such that molecular mass flux makes the bulk concentration decrease faster[3] than the temperature, and hence also the solubility.

Direct correlations between Reynolds number and convection coefficient was not obtained, but Figure 7 illustrates how the boundary layer, together with convective coefficients changes when flowing over a flat plate, i.e. moving into different flow regimes. It gives us an impression of the functions $h_m(Re_D)$ and $h(Re_D)$. When we move into different flow regimes, the shape of the

[3] Since wax deposition happens so slowly, the flow conditions can be considered stationary, $\frac{\partial}{\partial t} \cong 0$, and there are no changes with respect to time. The term "faster" here denotes the amount of variation in the flow direction.

curves changes. Thus, the magnitude of one coefficient compared to the other can differ between different regimes. This hypothesis is supported by the observations that bulk precipitation does not occur under laminar flow, only in turbulent. The illustration in Figure 7 is only valid for ordinary boundary layer. As mentioned, because bulk precipitation influences the shape of the concentration profile, the curve must therefore be determined by equations such as (4.7). As mentioned, observations have shown that k_r changes for different flow conditions. [4] It supports the hypothesis that flow rate effects bulk precipitation. A comment on k_r's dependency on Re_D is though lacking in the report.

5 CONCLUSION

The concentration profile is strongly dependent of the rate of bulk precipitation of wax. Accounting for bulk precipitation should therefore be included in order to obtain an accurate measure of the molecular mass flux of wax towards the wall. The preliminary best model is the MWP.

A theoretical concept of bulk precipitation optimizing is introduced and its existence is attempted validated mathematically. The optimum's existence is strongly supported by bulk precipitations flow condition dependency, reported by Singh et. al [4]. A dependency with Re_D is still missing. The concept should be considered highly theoretical and not necessarily a practical applicability. Cold flow concept serves the same purpose and the advantageous effect is much bigger, since all precipitated wax particles is suspended in the flow before the pipeline's entry.

6 FIGURES

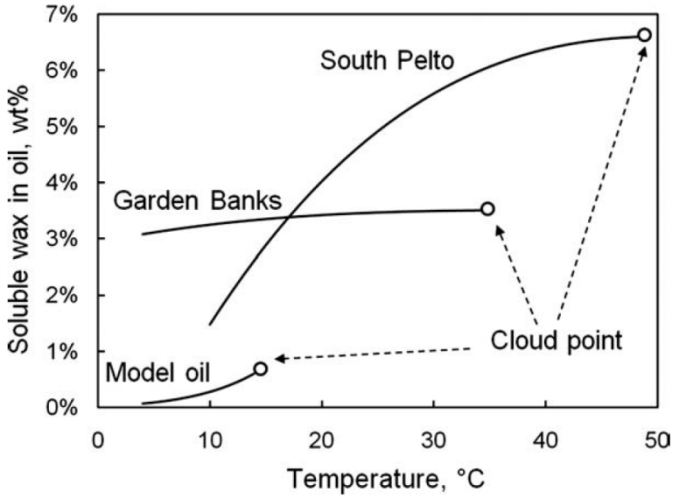

FIGURE 1: SOLUBILITY CURVES FOR DIFFERENT CRUDES. [4]

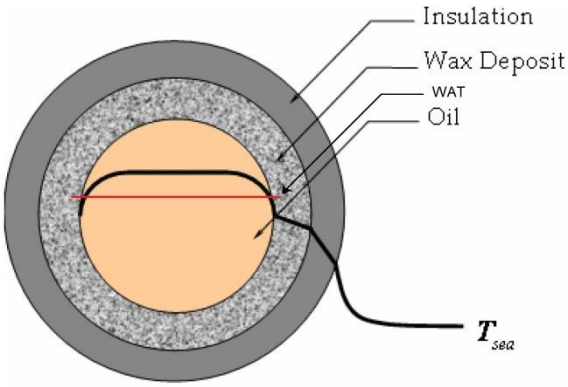

FIGURE 2: PIPE TEMPERATURE PROFILE.

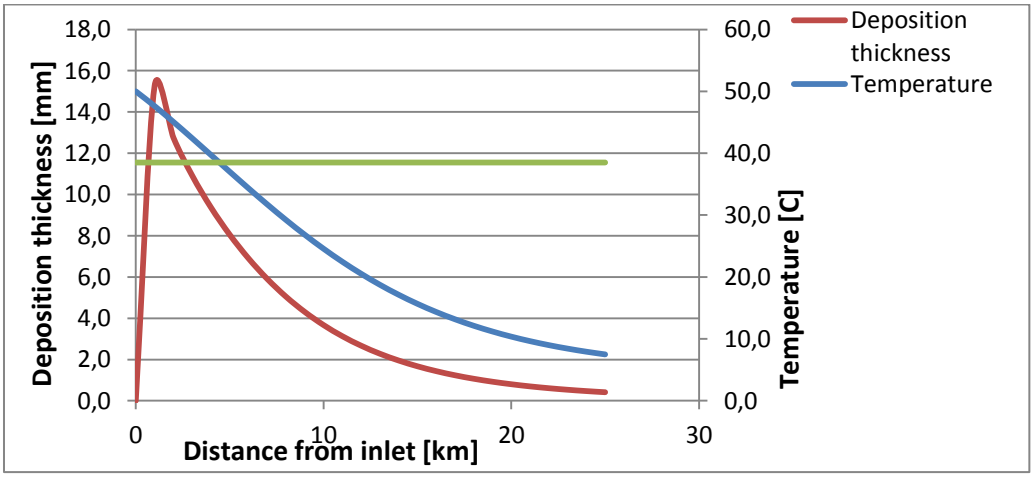

FIGURE 3: TEMPERATURE PROFILE AND DEPOSITION THICKNESS AFTER TWO WEEKS OF OPERATION, SIMULATIONS DONE IN HYSYS

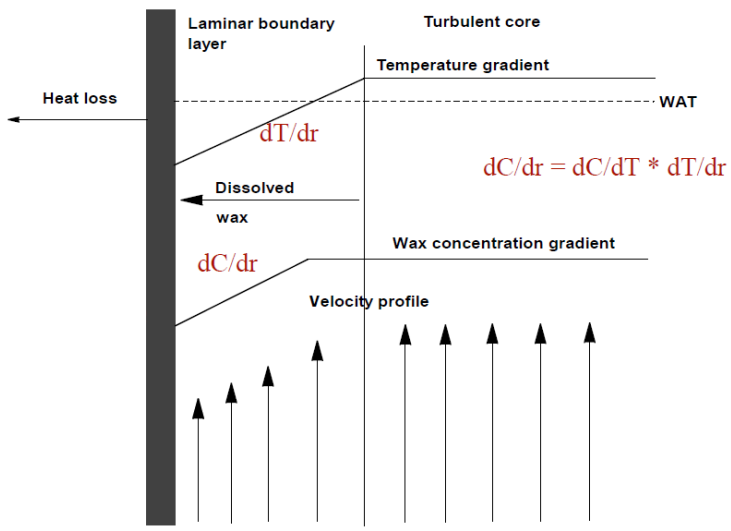

FIGURE 4: TEMPERATURE- AND CONCENTRATION PROFILE ILLUSTRATION [10, P. 14]

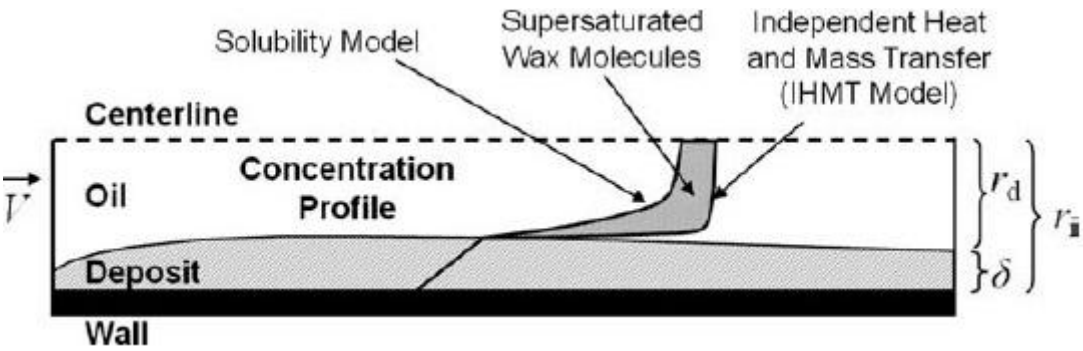

FIGURE 5: UPPER AND LOWER LIMIT FOR THE CONCENTRATION GRADIENT [4]

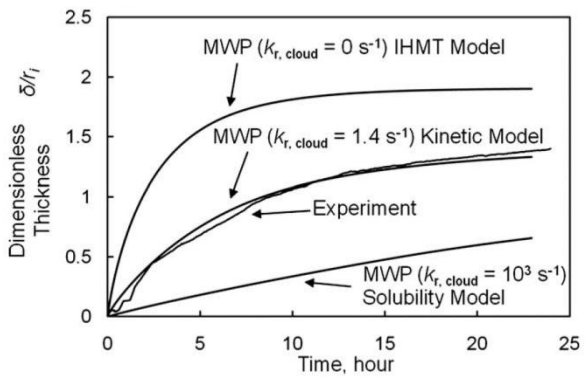

FIGURE 6: MINIMIZING THE EXPERIMENT-SIMULATION DEVIATION TO OBTAIN K_R. [4]

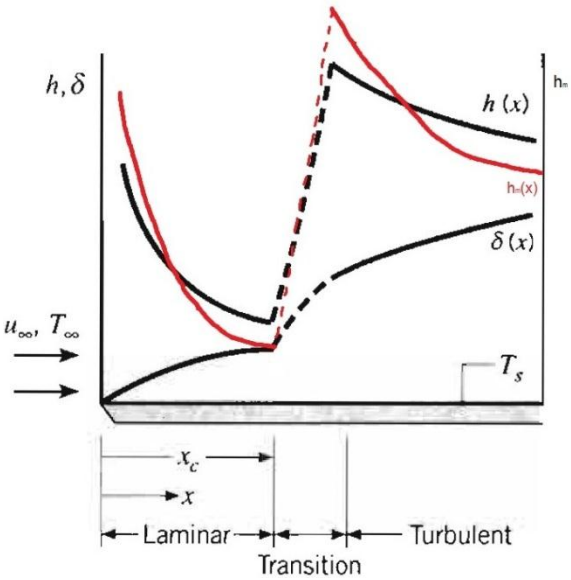

FIGURE 7: VARIATION OF VELOCITY BOUNDARY THICKNESS TOGETHER WITH CONVECTIVE HEAT- AND MASS TRANSFER COEFFICIENT FOR A FLOW OVER A FLAT PLATE. THE CURVE OF THE CONVECTIVE MASS TRANSFER COEFFICIENT WAS NOT ORIGINALLY DRAWN IN THE FIGURE, SO A POSSIBLE CURVE WAS DRAWN. [3, P. 337]

Appendix A DERIVATION OF THE SOLUBILITY METHOD

In order to fulfill the laws of energy and mass conservation, the heat and mass transfer done by advection must equal the conductive heat and mass transfer at the wall. Conduction at the wall is determined by equations (1.5) and (1.6), excluding the eddy diffusivities. Combining these with the equation for convective heat- and mass transport, (1.3) and (1.4), we obtain:

For heat transfer:

$$h\Delta T = -k \left.\frac{dT}{dr}\right|_{wall} \tag{A.1}$$

And for mass transfer:

$$h_m \Delta C = -D_{wo} \left.\frac{dC}{dr}\right|_{wall} \tag{A.2}$$

By using the definitions of Nusselt- and Sherwood number we get the following equations:

$$Nu_D = \left.\frac{2r}{\Delta T}\left(-\frac{dT}{dr}\right)\right|_{wall} \tag{A.3}$$

$$Sh_D = \left.\frac{2r}{\Delta C}\left(-\frac{dC}{dr}\right)\right|_{wall} \tag{A.4}$$

We divide the two equations on each other:

$$\frac{Sh_D}{Nu_D} = \frac{\left.\frac{dC}{dr}\right|_{wall}}{\left.\frac{dT}{dr}\right|_{wall}} \frac{\Delta T}{\Delta C} \tag{A.5}$$

The concentration at the wall-fluid interface can be calculated as a function of temperature: C=f(T). And by using the chain rule on equation (A.5) we obtain the following equation for the dimensionless convective mass transfer coefficient:

$$Sh_D = Nu_D \left(\frac{dC_{wo}(T)}{dT}\right) \frac{T_{bulk} - T_{wall}}{C_{wo,bulk}(T) - C_{wo,wall}(T)} \tag{A.6}$$

Appendix B TEMPERATURE DEPENDENCY OF VISCOSITY

In chapter 3.3 we are trying to derive a quantitative measure of bulk precipitation of wax particles. In order to do it correctly a temperature dependent equation for the diffusion coefficient, hence also viscosity, is needed. This appendix shows the correlations used for the equations in 3.3.

From everyday experience we know that the viscosity of a substance decreases drastically with increasing temperature. Viscosity is a measure of a fluids resistance to flow. It is a result of the cohesive forces (forces of attraction) between the molecules in the fluid. As the temperature increases, molecules moves faster and the amount of time molecules stays "in contact" with each other becomes less. Thus, these cohesive forces become smaller compared to the molecular momentum transfer between molecules and the viscosity is reduced. [11]

Svante Arrhenius developed an equation to describe temperature dependence of a chemical reaction constant. Both viscosity and the speed of a chemical reaction is determined by the interactions between molecules (or reactants), therefore this equation has also shown to be valid for the temperature dependency of viscosity. The equation he introduced is: [12]

$$k = A_r \exp\left(\frac{-E}{RT}\right) \tag{B.1}$$

A is the pre-exponential factor and the latter is basically the Boltzmann factor, where E is activation energy and R is the universal gas constant. For viscosity:

$$\mu = A_\mu \exp\left(\frac{E}{RT}\right) \tag{B.2}$$

Where A_μ is a viscosity coefficient for the respective material. The inversion of the Boltzman factor is due to the fact that less molecular interactions give higher viscosity. Since we are only interested in the viscosity dependency from a reference viscosity we can divide two copies of equation (B.2) at different temperatures on each other and we obtain:

$$\mu = \mu_{cloud} \exp\left[\frac{E}{R}\left(\frac{1}{T} - \frac{1}{T_{cloud}}\right)\right] \tag{B.3}$$

Appendix C DIFFUSION COEFFICIENT AND ITS TEMPERATURE- AND VISCOCITY DEPENDENCY

The diffusive mass flux is dependent of the solvents temperature and viscosity. This is reflected through the diffusion coefficient which correlation is described in this appendix. A high viscosity means that the cohesive forces between molecules are significant, which makes it more difficult for molecules to move. That is due to more molecular activity and the diffusion may happen faster.

There has been developed a many empirical correlations trying to describe the dependency, and the equation for chemical reaction constant which was used for the viscosity can also be used for the diffusion coefficient. In the SPE-literature especially two equation stand out:
Wilke& chang(1955): [13]

$$D_{AB} = 7.4 \cdot 10^{-8} \frac{(xM)^{1/2} T}{\mu V_{bp}^{\ 0.6}} \tag{C.1}$$

And Hayduk Minhas(1982): [14]

$$D_{AB} = 13.3 \cdot 10^{-8} \frac{T^{1.47} \mu^{\gamma}}{V}, \quad \gamma = \frac{10.2}{V} - 0.791 \tag{C.2}$$

x is an association parameter, multiple of nominal molecular weight of solvent to give effective value. M is the molecular weight, μ is the viscosity of solution, V is the molar volume of solute and V_{bp} is the molar volume at normal boiling point.

Typical values of the diffusion coefficient in hydrocarbons are in the range $10^{-10} < D_{AB} < 10^{-8}$ [2]

It seems reasonable to believe that the diffusion coefficient is impacted by the amount of suspended particles in the flow. As mentioned, if a transport mechanism for transportation of solid particles towards the wall do not exist, solid wax particles will stay in the flow and perhaps obstruct diffusion of molecules. No such correlation was found.

7 BIBLIOGRAPHY

[1] T. S. Brown, V. G. Niesen and D. D. Erickson, "Measurement and prediction of the kinetics of paraffin deposition," 1993.

[2] J. S. Gudmundsson, Flow Assurance, Solids in Oil and Gas Production, 2010.

[3] "Fundamentals of Heat and Mass Transfer," in *Fundamentals of Heat and Mass Transfer*, 5 ed., 2002.

[4] Z. Huang, H. S. Lee, S. H. Fogler and M. Senra, "A fundamental model of wax deposition in subsea oil pipelines," 2011.

[5] in *Transport Processes and Separation Process Principles*, 4 ed., 2003, pp. 403 - 404.

[6] E. R. Van Driest, "On turbulent flow near a wall," *Aerospace Science and technology,* vol. 23, pp. 1007-1011, 1956.

[7] M. S. Bhatti and R. K. Shah, in *Handbook of Single-Phase Convective Heat Transfer*, New York, Wiley-Interscience, 1987.

[8] R. Venkatesan, P. Singh and S. H. Fogler, "Formation and aging of incipient thin film wax oil gels," 2000.

[9] R. Venkatesan and S. H. Fogler, "Comments on analogies for correlated heat and mass transfer," 2004.

[10] N. Aske, *WAX - A flow assurance challange,* 2007.

[11] H. Khemani, "Brighthub," [Online]. Available: http://www.brighthub.com/engineering/mechanical/articles/10873.aspx. [Accessed 2008].

[12] A. D. McNaught and A. Wilkinson, IUPAC Compendium of Chemical Terminology, 2 ed., International Union of Pure and Applied Chemistry, 1997.

[13] C. R. Wilke and P. Chang, "Correlation of Diffusion Coefficients in Dilute Solutions," 1955.

[14] W. Hayduk and B. S. Minhas, "Correlations for prediction of molecular diffusivities in liquids," 1982.

[15] J. S. Weingarten and J. A. Euchner, "Methods for Predicting Wax Precipitation and Deposition," 1988.

[16] R. Venkatesan and J. L. Creek, "Wax deposition During Production Operations SOTA," 2007.

[17] O. B. Rygg, A. K. Rydahl and H. P. Rønningsen, "Wax deposition in offshore pipeline systems," 1998.

[18] K. Rosvold, "Wax Deposition Models," 1998.

[19] S. Pan, J. Zhu, D. Zhang, A. Razouki, M. Talbot and S. Wierzchowski, "Case studies on simulation of wax deposition in Pipelines," 2009.

[20] A. K. Mehrotra and H. O. Bidmus, "Heat-Transfer Calculations for Predicting Solids Deposition in Pipeline Transportation of “Waxy” Crude Oils," 2004.

[21] B. Edmonds, T. Moorwood, R. Szczepanski and X. Zhang, "Simulating Wax Deposition in Pipelines for Flow Assurance," 2007.

[22] E. D. Burger, T. K. Perkins and J. H. Striegler, "Studies of wax Deposition in the Trans Alaska Pipeline," 1981.

[23] H. O. Bidmus and A. K. Mehrotra, "Heat-Transfer Analogy for Wax Deposition from Paraffinic Mixtures," 2003.

[24] E. Wimmer, W. Wolf, J. Strict and P. Saxe, "Temperature-Dependent Diffusion Coefficients from ab initio Computations: Hydrogen in Nickel," 2006.

8 NOMENCLATURE

A	-	Constant for correlation of eddy viscosity
A_r	-	Pre-exponential factor (s^{-1})
A_μ	-	Viscosity coefficient (Pa s)
C	-	Concentration (kg/m^3)
C_w	-	Concentration of wax in oil or condensate
C_{wo}	-	Solubility of wax in oil (kg/m^3)
C_p	-	Oil Specific heat capacity (J/K/kg)
C_m	-	Cross sectional average concentration (kg/m^3)
C_s	-	Concentration at surface
D	-	Pipe inner diameter (m)
D_{AB}	-	Diffusion coefficient of material A in solvent B (m^2/s)
D_{wo}	-	Binary diffusion coefficient of wax in oil (m^2/s)
E	-	Chemical reaction activation energy (kJ/mol)
$f(x_1,x_2,...x_n)$	-	An undefined function of variables $x_1,x_2...x_n$.
G	-	Growth rate of precipitated wax particles ($kg/m^3/s$)
G_L	-	Growth rate per unit length (kg/s/m)
G_{tot}	-	Total growth rate of solid particles (kg/s)
h	-	Convective heat transfer coefficient ($W/m^2/K$)
h_m	-	Convective mass transfer coefficient (m/s)
k	-	Chemical reaction constant in equation (B.1)
k_r	-	Precipitation rate constant (1/s)
$k_{r,cloud}$	-	Precipitation rate constant at WAT(1/s)
k_f	-	Thermal conductivity of oil (W/(m k))
L	-	Distance from inlet (m)
L_{tot}	-	Total length of pipeline (m)
$\dot{m}$	-	Pipe mass flow rate (kg/s)
n''	-	Mass flux per unit area(kg/m^2)
P	-	Periphery, $2\pi r$ (m)
q''	-	Heat flux (W/m^2)
q_L	-	Heat flux per unit length(W/m)
r	-	Radial distance from the pipe lateral axis (m)
r_p	-	Pipe inner radius (m)
r_{WAT}	-	Radial position of WAT (m)
T_L	-	Temperature at position L from inlet (C)
T_b	-	Bulk temperature (C)
T_u	-	Ambient temperature (C)
T_{core}	-	Volumetric, temporal average temperature of the turbulent core. (C)
T_m	-	Volumetric, temporal average temperature of total cross sectional area. (C)
T_1	-	Inlet temperature to the pipeline (C)
U	-	Heat transmission coefficient
u_τ	-	Friction velocity (m/s)

u(r)	-	Velocity at radial distance r from pipe axis (m/s)
V	-	Molecular volume of solute(cm^3/mol)
V_{bp}	-	Molecular volume at boiling temperature
V_z	-	Lateral velocity (m/s)
V_z^+	-	Non-dimensional velocity parallel to the wall
y^+	-	Non-dimensional wall normal distance
z	-	Lateral position (m)
ε	-	Momentum diffusivity (m^2/s)
ε_m	-	Eddy mass diffusivity (m^2/s)
ε_h	-	Eddy thermal diffusivity (m^2/s)
τ_w	-	Shear stress (N/m^2)
δ	-	Deposition thickness (m)
μ	-	Viscosity of solution (Pa s)
κ	-	Constant for the correlation of eddy viscosity in equation(1.9)
ρ	-	Fluid density (kg/m^3)
ν	-	Kinematic viscosity (m^2/s)

8.1.1 ABBREVIATIONS

SPE	-	Society of petroleum engineers
WAT	-	Wax appearance temperature
MWP	-	Michigan wax predictor

8.1.2 DIMENSIONLESS NUMBERS

The dimensionless numbers that are defined below are used to either calculate the convective heat and mass transfer coefficients, or to determine the dependency of one coefficient to another.

- Reynolds number, $\mathrm{Re}_D = \frac{VD}{\nu}$: Represents the ratio between inertia and viscous forces, and are used to describe flow conditions.
- Nusselt number, $Nu_D = \frac{hD}{k_f}$: Represents the ratio between the heat transfer by conduction and the heat transfer by convection. Often referred to as the dimensionless convective heat transfer coefficient.
- Sherwood number, $Sh_D = \frac{h_m D}{D_{wo}}$: Represent the ratio between the mass transfer by conduction and the mass transfer by convection. Often referred to as the dimensionless convective mass transfer coefficient.
- Prandtl number, $\mathrm{Pr} = \frac{C_p \mu}{k}$: Represent the ratio of momentum diffusivity and thermal diffusivity

- Schmidt number, $Sc = \frac{\nu}{D_{wo}}$: Represents the ratio between momentum diffusivity and mass diffusivity
- Lewis number, $Le = \frac{\alpha}{D_{AB}}$: Represents the ratio between thermal diffusivity and mass diffusivity.